Eckhaus Instability in Laser Cavities with Harmonically Swept Filters

Feng Li, *Member, IEEE, Senior Member, OSA,* Dongmei Huang, K. Nakkeeran, J. Nathan Kutz, Jinhui Yuan, *Senior Member, IEEE, Senior Member, OSA,* and P. K. A. Wai, *Fellow, IEEE, Fellow, OSA*

***Abstract*—In this paper, we report the existence of Eckhaus instability in laser cavities with harmonically swept filters, of which Fourier Domain Mode Locked (FDML) laser is an important example. We show that such laser cavities can be modeled by a real Ginzburg Landau equation with a frequency shifting term arisen from the cavity dispersion. We analytically derived a solution of the governing equation and analyzed its stability. We found that the cavity dispersion introduces a continuous frequency shift to the laser signal such that it will be eventually pushed outside the stable region and trigger the Eckhaus instability. We show that the repeated triggering of the Eckhaus instability in the laser cavities is the dominant effect that leads to the high frequency fluctuations in FDML laser output, which is the unique feature of such laser cavities and intrinsically limits the signal quality of the FDML lasers with nonzero cavity dispersion.**

***Index Terms*—Eckhaus instability, Real Ginzburg Landau equation, Swept laser, Fourier domain mode locking.**

I. Introduction

Optical signals in laser cavities are stabilized by constraints either in time domain or frequency domain, or their combination. A continuous wave (CW) single frequency laser is obtained when a narrow bandpass optical filter is introduced in the cavity if no other physical effects influence the signal in the time domain. Whereas, mode-locked lasers that generate ultrashort pulses are designed by adding temporal light constraining elements such as an intensity modulator or nonlinear loss elements such as a saturable absorber to the laser cavity. In traditional laser cavities, the constraints in time and frequency domains are realized by different optical components. In 2005, a novel type of laser with an intracavity swept filter driven at a harmonic resonant frequency of the laser cavity, namely Fourier domain mode locked (FDML) laser, is proposed and demonstrated experimentally [1], [2]. The FDML laser was proposed to break the bottleneck of sweep rate caused by the signal build up time in conventional short cavity swept laser cavities, to meet the requirement in the fast growing application of optical coherence tomography (OCT) [3]–[5]. Since the long fiber cavity of FDML lasers could buffer the entire swept signal in the cavity to avoid the rebuilding of laser signal, the wavelength sweep rate can be enhanced to MHz level [6], [7].

The working principle of an FDML laser is radically different from either a single frequency laser or a mode locked laser. In an FDML laser cavity, the swept filter constrains the intracavity laser signal in both the time and frequency domains simultaneously. If we observe the signal within a narrow bandwidth in the sweep range, the swept filter will introduce a temporal window function for the specific frequency of the signal. The duration of the window function is much shorter than the cavity round trip time. Thus the sweeping filter provides a periodic and narrow temporal confinement to any given single wavelength of the signal, but the temporal positions of the window function are different for different wavelengths of the signal. On the other side, if we observe the cavity in a short period of time, the bandpass filter provides a narrow spectral confinement to the signal, while the central wavelength of this spectral confinement varies periodically with time.

Ideally, a laser with a harmonically swept filter should repeatedly output a chirped signal with continuously varying carrier frequency and a constant or smoothly varying intensity profile. But the performance of the realized laser, e.g. an FDML laser, is far from the ideal output. Although FDML lasers have been deployed in OCT systems as the swept sources, the signal quality is limited by its large instantaneous linewidth [8]–[10], which manifested as high frequency fluctuations on the temporal waveforms. A theoretical model considering dispersion, Kerr nonlinearity, gain saturation and spectral filtering has been proposed to investigate the signal dynamics in the FDML laser cavity [11], [12]. Although

This work was supported in part by National Key R&D Program of China (2019YFB1803904), in part by Science, Technology and Innovation Commission of Shenzhen Municipality (SGDX2019081623060558), in part by Research Grants Council, University Grants Committee of Hong Kong SAR (PolyU152241/18E), and in part by Guangdong Basic and Applied Basic Research Foundation (2021A1515012544) (*Corresponding author: Dongmei Huang).*

Feng Li and P. K. A. Wai are with the Photonics Research Centre, Department of Electronic and Information Engineering, The Hong Kong Polytechnic University, Hung Hom, Hong Kong SAR, China, and The Hong Kong Polytechnic University Shenzhen Research Institute, Shenzhen 518057, China. P. K. A. Wai is also with the Department of Physics, Hong Kong Baptist University, Kowloon Tong, Hong Kong SAR, China (e-mail: lifeng.hk@gmail.com; alexwai@hkbu.edu.hk).

Dongmei Huang is with the Photonics Research Centre, Department of Electrical Engineering, The Hong Kong Polytechnic University, Hung Hom, Hong Kong SAR, China, and The Hong Kong Polytechnic University Shenzhen Research Institute, Shenzhen 518057, China (e-mail: meihk.huang@polyu.edu.hk).

K. Nakkeeran is with the School of Engineering, Fraser Noble Building, University of Aberdeen, Aberdeen AB24 3UE, UK (e-mail: k.nakkeeran@abdn.ac.uk).

J. Nathan Kutz is with the Department of Applied Mathematics, University of Washington, Seattle, WA 98195-2420, USA (e-mail: kutz@uw.edu).

Jinhui Yuan is with the State Key Laboratory of Information Photonics and Optical Communications, Beijing University of Posts and Telecommunications, Beijing 100876, China and the Research Center for Convergence Networks and Ubiquitous Services, University of Science & Technology Beijing, Beijing 100083, China (e-mail: yuanjinhui81@163.com).

Manuscript received Nov 01, 2020; revised xxx xx, 2021.

the impact of each individual elements in the cavity was investigated by numerical simulations, the origin and cause of the high frequency fluctuations have not been investigated. The instabilities arising in the FDML laser cavities have been investigated with a set of delayed differential equations [13] and the existence of localized coherent structures including Nozaki-Bekki holes have been discussed [14]. Besides the theoretical investigation, quasi-stationary solutions with high coherence have been demonstrated when the cavity dispersion is compensated to nearly zero [15]. The experimental results strongly indicate that the cavity dispersion is the dominating effect that determines the stability of solutions in FDML lasers.

In this paper, we investigate the intrinsic stability of laser cavities with harmonically swept filters by studying the signal dynamics with a governing equation after peeling off the auxiliary effects which are either minor or optional in such laser cavities. A quasi-stationary analytical solution is presented for the first time and the stability of which is also investigated.

II. Theoretical Formalism

In practical FDML lasers, the swept filter is typically driven to sweep in a range of several THz with a period of several microseconds. Because of the large time-bandwidth product ($\sim 10^7$) of the frequency swept signal, it is difficult to model the signal dynamics in the laboratory frame. By converting the description of system to a reference frame co-moving with the swept filter, a theoretical model has been proposed [11], [12]

$$\begin{aligned}\partial_z u =& g(u,\omega_s)(1-i\alpha)u - \sigma u - a(i\partial_t)u \\ &+ iD_2\omega_s^2(t)u + iD_3\omega_s^3(t)u + i\gamma|u|^2u - iD_2\partial_t^2 u,\end{aligned} \tag{1}$$

where u is the complex amplitude in the filter frame defined as $u = A\exp(i\int^t \omega_s(t')dt')$, $\omega_s(t)$ is the instantaneous center frequency of the sweeping filter and A is the complex amplitude of the signal in the laboratory frame. The first term in RHS describes the saturated gain g and the linewidth enhancement factor α of a semiconductor optical amplifier (SOA). Since the fluctuations of FDML laser output is normally limited in the band of several GHz, the dynamics of α is not considered [16]. The model also includes the linear loss σ, second order dispersion D_2, third order dispersion D_3 and Kerr nonlinearity γ of the fiber cavity, and the steady filtering profile $a(i\partial_t)$ of the sweeping filter. The last term $-iD_2\partial_t^2 u$ describes the second order dispersion that falls within the filter bandwidth, i.e. the in-band dispersion.

Equation (1) has been applied in the numerical simulations of FDML lasers to investigate the signal evolution and quality [11], [12]. Simulation results show that the signal quality is degraded by multiple factors. The fiber dispersion breaks down the synchronization between the filter and the signals because of the different round trip time of different wavelengths [8], [11]. The linewidth of the signal is increased by the fiber nonlinearity and the linewidth enhancement factor of SOA [12]. Although investigations by turning on and off of specific physical effects in simulations can provide some intuitive understanding of the cavity dynamics, they cannot describe the interaction between different effects and cannot reveal the nature of the underlying dynamics. For example, high frequency fluctuations on the signal waveforms were observed in the numerical simulations of Eq. (1), but the mechanism to generate these high frequency fluctuations is unknown, let alone the method to avoid them. In Fig. 1(a), a typical raw waveform of the signal in an FDML laser cavity modeled by Eq. (1) is shown as the blue curve. Fig. 1(a) plots a 1 km fiber cavity with a round trip time of 5 μs. The fiber dispersion coefficients are $D_2 = -1.0$ ps^{2}km^{-1} and $D_3 = 0.02$ ps^{3}km^{-1}. The nonlinear coefficient $\gamma = 2.0$ W^{-1}km^{-1}. The gain is modeled as a lump element with a power gain of $G = [G_0(\omega_s)/(1+|u(t)|^2/I_{sat})]^{1-i\alpha}$, where the saturation power $I_{sat} = 1$ mW, the linewidth enhancement factor $\alpha = 5$, and the small signal gain $G_0(\omega_s) = 150/(1+\omega_s^2/\omega_g^2)$ with $\omega_g = 40$ ps^{-1}. The linear loss coefficient $\sigma = 0.5$ km^{-1} also includes the insertion loss of other elements in the cavity. The swept filter is modeled by the intensity transfer function with a Gaussian profile $T_f(\omega) = \exp(-\omega^2/\omega_f^2)$, where the filter bandwidth $\omega_f = 0.04$ ps^{-1}. The sweeping function of the filter is modeled by $\omega_s(t) = \omega_m\cos(2\pi f_0 t)$, where $\omega_m = 40$ ps^{-1} and $f_0 = 200$ kHz. The inset of Fig. 1(a) shows the zoom-in detail of the waveforms, where the high frequency fluctuation is clearly shown on the raw waveform. These fluctuations dominate the signal and hence the waveform is usually averaged with adjacent signals in a range of several nanoseconds to obtain a smooth waveform, e.g., the red curve in Fig. 1(a) [11], [12].

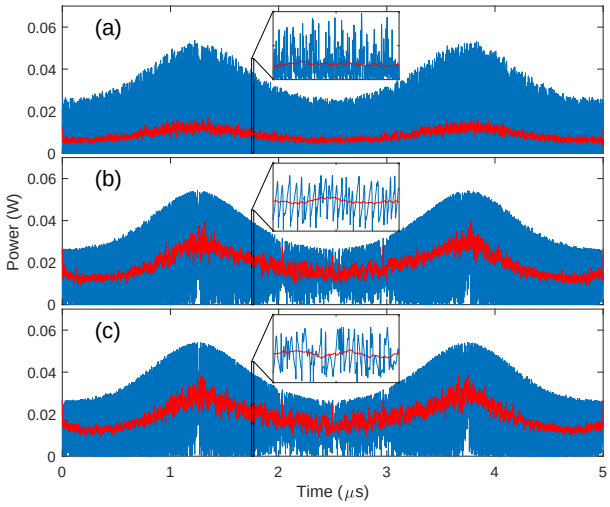

Fig. 1. The waveforms of signals in FDML laser cavities modeled by (a) Eq. (1), with $\alpha = 5$, (b) Eq. (1), with $\alpha = 0$, and (c) Eq. (2), respectively. The blue and red curves are the raw and smoothed waveforms respectively. The insets show the zoom-in detail of the waveforms in the interval $t \in [1.7\ \mu\text{s}, 1.72\ \mu\text{s}]$.

A. Reduction of theoretical model

From the simulation results, it is likely that Eq. (1) has neither an analytical solution nor a steady state solution. A likely reason of the presence of the high frequency components in the signal is the onset of an instability in the cavity dyanmics, which severely affects the signal quality. To delineate the intrinsic reason of the noiselike fluctuations, we simplify the

cavity model for a systematic analysis to find out the reason and source of the signal instability.

First, we consider the contribution of the linewidth enhancement factor which plays an important role in the signal quality of laser cavities with SOAs. Figure 1(b) shows the intracavity signal modeled by Eq. (1) with the linewidth enhancement factor α set to zero, i.e. $\alpha = 0$. We note that the waveform still exhibits very complex fluctuations although the inset shows a lower oscillation frequency compared with that of Fig. 1(a). It is therefore clear that while the linewidth enhancement factor degrades the signal quality in FDML laser cavities with SOAs, it is not the intrinsic source of the instability in such cavities. Thus for simplicity, in the subsequent analysis we drop the effect of the linewidth enhancement factor from the laser model of Eq. (1). By using the Wentzel–Kramers–Brillouin (WKB) analysis [17], we found that the nonlinear phase shift and in-band dispersion play a minor role and these terms are therefore neglected in the first order approximation [18]. Thus Eq. (1) can be reduced to

$$\begin{aligned}\partial_z u = \; & g(u,\omega_s)u - \sigma u - a(i\partial_t)u \\ & + iD_2\omega_s^2(t)u + iD_3\omega_s^3(t)u.\end{aligned} \tag{2}$$

Fig. 1(c) dispict the simulation results of the simplified equation (2), which resemble that of Fig. 1(b) which is obtained with the full equation (1) and $\alpha = 0$, except minor differences shown in the insets which are the zoom-in of the signals.

We then neglect the wavelength dependence of the gain and assume a Gaussian spectral filter with a bandwidth ω_f, Eq. (2) is then further simplified as

$$\begin{aligned}\partial_z u = \; & gu - \sigma u + \tfrac{1}{2}\omega_f^{-2}\partial_t^2 u \\ & + iD_2\omega_s^2(t)u + iD_3\omega_s^3(t)u,\end{aligned} \tag{3}$$

where $g(u) = g_0/(1 + |u|^2/I_{sat})$ is the saturated gain coefficient. The delayed response of gain [11], [19] is not considered since it does not dominate the instability. The simulation results of the simplified model of Eq. (3) capture most of the signal dynamics of the FDML laser system, especially the high frequency intensity fluctuations of the waveform.

The gain saturation factor is then expanded in Taylor series of $|u|^2$. By keeping only the first order term, Eq. (3) is reduced to

$$\begin{aligned}\partial_z u = \; & (g_0 - \sigma)u - g_0 I_{sat}^{-1}|u|^2 u + \tfrac{1}{2}\omega_f^{-2}\partial_t^2 u \\ & + iD_2\omega_s^2(t)u + iD_3\omega_s^3(t)u.\end{aligned} \tag{4}$$

Eq. (4) can be normalized to

$$\partial_Z U = U - |U|^2 U + \partial_T^2 U + i\epsilon^{-1}C(\epsilon T)U, \tag{5}$$

by defining normalization of variables as

$$\begin{aligned}& U = u\sqrt{g_0/[2(g_0-\sigma)I_{sat}]}\,, \\ & Z = z(g_0 - \sigma), \\ & T = t\omega_f\sqrt{2(g_0-\sigma)}, \\ & \Omega = \omega/[\omega_f \times \sqrt{2(g_0-\sigma)}\,], \\ & C(\epsilon T) = \epsilon\left[S_2\Omega_s^2(T) + S_3\Omega_s^3(T)\right], \\ & S_2 = D_2\omega_f^2\sqrt{8(g_0-\sigma)^3 I_{sat}/g_0}\,, \\ & S_3 = D_3\omega_f^3 4(g_0-\sigma)^2\sqrt{I_{sat}/g_0}\,,\end{aligned} \tag{6}$$

where the time scaling factor ϵ is defined as the inverse of the normalized time window or round trip time of the laser cavity.

Equation (5) is a real Ginzburg Landau equation (RGLE) with a chirp phase term C contributed by the dispersion in the fiber cavity. In a dispersion-less laser cavity, Eq. (5) will reduce to a standard RGLE as

$$\partial_Z U = U - |U|^2 U + \partial_T^2 U. \tag{7}$$

RGLE has been extensively studied in fluid dynamics. More importantly, stationary solutions are available for the system governed by the RGLE which are single frequency continuous waves. The stationary solution for Eq. (7), with normalized angular frequency Ω is

$$U = \sqrt{1-\Omega^2}e^{-i\Omega T}, \tag{8}$$

which is nontrivial in the frequency region $|\Omega| < 1$. But the stationary solutions are unstable when $\Omega^2 > 1/3$, which is known as the *Eckhaus instability*. Eckhaus instability was first discussed in 1960s in the modeling of convection in fluid systems governed by the RGLE [20]. Within a short span of time, interest on the instability has moved to systems described by the complex Ginzburg Landau equation (CGLE), which is the modulation instability, where the Eckhaus instability can be treated as a speical case with the imaginary terms set to zero [21]. As a reduced form of CGLE, nonlinear Schrödinger equation (NLSE) has attracted more attention than the RGLE because of the existence of the analytical solitary solution, especially after soliton was reported in optical fibers by Hasegawa and Tappert [22]. For the NLSE, the modulation instability of optical continuous wave has been very well studied. In systems with dissipative and gain elements, such as laser cavities, the more general CGLE is adopted to model the nonlinear pulse dynamics in the cavity [23]–[25]. But in all those studies, the nonlinear phase shift and dispersion were considered as the dominant effects in pulse shaping and stable propagation. Although RGLE is seldom used to describe an optical system, Eckhaus instability has also been discussed when considering the spatial effects or a delayed feedback in lasers [26]–[29]. However, in an one dimensional cavity, where spatial effects and delay are not significant in laser system dynamics, the Eckhaus instability does not show up as a dominating effect.

B. Solution and stability analysis

Equation (5) is an initial value problem, the evolution of the signal can be solved if the initial field is given. We note that Eq. (5) does not possess stationary solutions because of the existence of a nonzero phase term. To solve Eq. (5), we introduce an amplitude-phase transformation of the form

$$\bar{U} = U\exp[-i\epsilon^{-1}C(\epsilon T)Z]. \tag{9}$$

Eq. (5) is transformed to

$$\begin{aligned}\partial_Z \bar{U} = \; & \bar{U} - |\bar{U}|^2\bar{U} + \partial_T^2\bar{U} - C'^2 Z^2\bar{U} \\ & + 2iC'Z\partial_T\bar{U} + i\epsilon C''Z\bar{U},\end{aligned} \tag{10}$$

where $C' = \partial_{\epsilon T}C$ and $C'' = \partial_{\epsilon T}^2 C$. We then split the temporal dynamics by fast time $t_1 = T$ and slow time $t_2 = \epsilon T \in [0, 1]$,

and assume a polynomial expansion of $\bar{U} = \bar{U}^0 + \epsilon\bar{U}^1 + \epsilon^2\bar{U}^2 + \cdots$, where $\bar{U}^{\mathrm{n}}$ is the n-th order solution. By grouping the equation in polynomial order of ϵ, the governing equation at zero-th order of ϵ can be derived as

$$\begin{aligned}\partial_Z\bar{U}^0 = \; & \bar{U}^0 - \left|\bar{U}^0\right|^2\bar{U}^0 + \partial_{t_1}^2\bar{U}^0 \\ & - C'^2Z^2\bar{U}^0 + 2iC'Z\partial_{t_1}\bar{U}^0.\end{aligned} \tag{11}$$

By assuming $\bar{U}^0 = X(z,t_2)\exp\left[-i\bar{\Omega}_0(t_2)t_1\right]$, where X and $\bar{\Omega}_0$ are real, Eq. (11) could be transformed into a real equation

$$\partial_Z X = X - X^3 - \left[\bar{\Omega}_0(t_2) - C'Z\right]^2 X. \tag{12}$$

Letting $I = X^2 \neq 0$, Eq. (12) is reduced into a Riccati equation

$$\partial_Z I = R(Z)I - 2I^2, \tag{13}$$

where $R(Z) = 2\left[1 - \left(\bar{\Omega}_0(t_2) - C'Z\right)^2\right]$. By solving the Riccati equation (13), the evolution of the signal along Z governed by Eq. (11) can be obtained as

$$\bar{U}^0(Z) = \frac{\exp(-i\bar{\Omega}_0(t_2)t_1)}{\sqrt{I_0^{-1}e^{Q(0)-Q(Z)} + 2\int_0^Z e^{Q(x)-Q(Z)}dx}}, \tag{14}$$

where I_0 and $\bar{\Omega}_0(t_2)$ are the intensity and instantaneous frequency of $\bar{U}^0$ at $Z = 0$, and $Q(Z) = \int_0^Z R(x)dx$. For simplicity in the notation, we will write $\bar{U}^0$ as $\bar{U}$ in the following discussion.

The linear stability of the solution (14) can be investigated by assuming a perturbation $a(t_1,t_2)$ of the solution at $Z = Z_0$ as $W(Z_0) = \bar{U}(Z_0)(1+a)$. The evolution of the perturbed solution is assumed as

$$W(Z,t_1,t_2) = \bar{U}(Z,t_1,t_2)[1 + e^{\Lambda(Z,t_2)}a(t_1,t_2)], \tag{15}$$

where $\partial_Z\Lambda = \lambda(Z,t_2)$ indicates the growth rate of the perturbation. If $\lambda(Z > Z_0, t_2) > 0$, the perturbation at time point t_2 will grow exponentially, thus the solution will become unstable. By substituting Eq. (15) into Eq. (11), the governing equation of the perturbation is calculated as

$$\begin{aligned}\lambda a\bar{U} = & -\left|\bar{U}\right|^2\bar{U}\left(a + a^*\right) + 2\partial_{t_1}a\partial_{t_1}\bar{U} \\ & + \bar{U}\partial_{t_1}^2 a + 2iC'Z\bar{U}\partial_{t_1}a.\end{aligned} \tag{16}$$

For the solution described by Eq. (14), where $\partial_{t_1}\bar{U} = -i\bar{\Omega}_0(t_2)\bar{U}$, the governing equation Eq. (16) will become

$$\lambda a = -I\left(a + a^*\right) + \partial_{t_1}^2 a + 2i\Omega_i\partial_{t_1}a, \tag{17}$$

where I is the intensity and $\Omega_i = C'Z - \bar{\Omega}_0(t_2)$ is the instantaneous frequency of U. Considering the coupling between the conjugated fields, the perturbed field can be written as

$$a(t_1,t_2) = \alpha_k(t_2)\exp(-ikt_1) + \beta_k(t_2)\exp(ikt_1), \tag{18}$$

where $k > 0$ is the mode number of the perturbation, and $\alpha_k(t_2)$ and $\beta_k(t_2)$ are real functions. Substitution of Eq. (18) into Eq. (17) gives the eigenequation of the perturbation modes as

$$\lambda\begin{pmatrix}\alpha_k\\ \beta_k\end{pmatrix} = -\begin{pmatrix}I + k^2 + 2k\Omega_i & I\\ I & I + k^2 - 2k\Omega_i\end{pmatrix}\begin{pmatrix}\alpha_k\\ \beta_k\end{pmatrix}. \tag{19}$$

α_k and β_k have nonzero solutions only when

$$\begin{vmatrix}I + k^2 + 2k\Omega_i + \lambda & I + \lambda\\ I + \lambda & I + k^2 - 2k\Omega_i + \lambda\end{vmatrix} = 0, \tag{20}$$

which has solutions $k = 0$, or $\lambda = 2\Omega_i^2 - I - k^2/2$ for $k > 0$. Clearly, λ will be negative for all $k > 0$ modes if $2\Omega_i^2 - I < 0$, which is the criterion for the stability of the solution. Thus, the stability condition for Eq. (14) is

$$\begin{aligned}\lambda_{max} = & \; 2\left(C'Z - \bar{\Omega}_0\right)^2 \\ & - \left[I_0^{-1}e^{Q(0)-Q(Z)} + 2\int_0^Z e^{Q(x)-Q(Z)}dx\right]^{-1} < 0.\end{aligned} \tag{21}$$

In Section III, we will discuss the solutions and their stability based on Eqs. (14) and (21).

C. Linewidth enhancement factor

If a semiconductor amplifier, like an SOA, is used in an FDML laser, then the linewidth enhancement factor of the semiconductor amplifier is another important factor that affects the performance of the FDML laser. If the linewidth enhancement factor is considered in the model in Section II-A, the reduced model Eq. (5) will become a complex Ginzburg Landau equation without intraband dispersion as

$$\partial_Z U = U - |U|^2U + i\alpha|U|^2U + \partial_T^2 U + i\epsilon^{-1}C(\epsilon T)U. \tag{22}$$

In a cavity with fully compensated dispersion, $C = 0$. The stationary solution of Eq. (22) is given by

$$U = \sqrt{1-\Omega^2}e^{-i\Omega T + i\alpha(1-\Omega^2)Z}, \tag{23}$$

which has an extra phase term $\alpha(1-\Omega^2)Z$ when compared with the solution (8). Although the extra phase term will not change the intensity profile or the center frequency of the solution, the stability region of the solution (23) is modified because the Eckhaus instability criterion has been changed to the Benjamin-Feir instability criterion as

$$\Omega^2 > \frac{1}{2\alpha^2 + 3}. \tag{24}$$

Considering a typical value $\alpha = 5$, the stationary solution will be stable only for $|\Omega| < 0.137$, which is narrower than the region $|\Omega| < 0.577$ with $\alpha = 0$. The narrowing of stable region by nonzero α will also be inherited to the evolving solution and the corresponding stable region. However, the nonzero α will not deviate a stationary solution from the stable region to the unstable region thus it is possible to obtain a high quality stationary solution in an FDML laser using SOA with nonzero α as gain element when the dispersion is fully compensated [15].

III. Results and discussion

In Section II, we have obtained the analytical solution and investigated the stability of the solution. In this Section, we will show how the high frequency fluctuations on the waveform of FDML lasers are generated. First we will show the triggering of Eckhaus instability in the simplest case of a frequency shifted stationary signal. Then the triggering of Eckhaus instability of a signal with a fixed chirp profile will be demonstrated. Finally, we explain the evolution of the onset of instability in a practical FDML laser cavity.

A. Frequency shifted stationary signal

In the simplest case, where $C' = 0$, Eq. (14) is reduced to

$$\bar{U}_0 = \sqrt{1 - \bar{\Omega}_0^2(t_2)}\exp\left[-i\bar{\Omega}_0(t_2)t_1\right]. \tag{25}$$

Also, Q is simplified to $Q(Z) = 2Z\left[1 - \bar{\Omega}_0^2(t_2)\right]$, and the stability criterion of the eigenvalue changes to $\lambda_{max} = 3\bar{\Omega}_0^2(t_2) - 1 < 0$, which is the condition for Eckhaus instability. Especially when $\bar{\Omega}_0(t_2)$ is a constant, the solution becomes the stationary solution of Eq. (8). Such stationary solution can be found in laser cavities modeled by RGLE. A nonzero relative frequency offset $\bar{\Omega}_0$ can be introduced either by a frequency shifter, or a fast tuning of the spectral filter in the cavity. The stability of the stationary signal depends on the offset frequency $\bar{\Omega}_0$, which can be divided into three regions, $\bar{\Omega}_0^2 < 1/3$, $1/3 \leq \bar{\Omega}_0^2 \leq 1$ and $\bar{\Omega}_0^2 > 1$. The frequencies $\bar{\Omega}_0^2 = 1/3$ and $\bar{\Omega}_0^2 = 1$ stand for the critical point to trigger the Eckhaus instability and the threshold frequency for positive net gain, respectively.

Figure 2 shows the spectra of signals with frequencies in the three different regions. In Fig. 2(a), the frequency $\bar{\Omega}_0 = 0.5$, which is within the stable region of $\bar{\Omega}_0^2 < 1/3$, the amplitude of the signal is -0.866 dB. The solution is stable. The sideband noise, which is due to the roundoff error of the computer, is lower than -200 dB at $Z = 50,000$. When $\bar{\Omega}_0$ increases to 0.6, which is inside the Eckhaus unstable region $1/3 < \bar{\Omega}_0^2 < 1$, sidebands are generated on both sides of the signal at $Z = 3,000$ as shown in Fig. 2(b). In this region, although the signal is unstable, the original single frequency signal decays very slowly until the sidebands grow to relatively large amounts. Fig. 2(d) shows the spectral evolution under Eckhaus instability. We observed sidebands, including higher order sidebands, are excited by the instability at very short distance. Eventually, the sideband at the low frequency side, which experiences higher net gain, replaces the original single frequency signal as the dominant mode. The new signal is stable as it is in the stable region of $\bar{\Omega}_0^2 < 1/3$. In other words, the original frequency which is in the Eckhaus unstable region is downshifted by the instability into the stable region. Finally, when $\bar{\Omega}_0$ is further increased to $\bar{\Omega}_0^2 > 1$, as shown in Fig. 2(c), the solution defined in Eq. (25) attenuated quickly while new signal builds up from noise.

B. Periodically chirped signal

In an FDML laser cavity, the cavity dispersion will introduce a time varying periodic chirp to the signal. Before considering the dynamic chirp caused by the $C'Z$ term, we first analyze the effect of a periodic chirp added to the signal. We consider a signal with a stationary sinusoidal chirp profile $\bar{\Omega}_0(t_2) = \bar{\Omega}_c - \bar{\Omega}_m \times \cos(2\pi t_2)$ in a cavity with $C' = 0$, where $\bar{\Omega}_c = 0.4$ and $\bar{\Omega}_m = 0.2$ are the center and amplitude of the frequency modulation, respectively. Since $\bar{\Omega}_0(t_2)$ is fully within the region of $\bar{\Omega}_0^2 < 1$, the solution given by Eq. (25) is still valid. The satisfaction of stable criterion $\lambda_{max} = 3\bar{\Omega}_0^2(t_2) - 1 < 0$ depends on the value of $\bar{\Omega}_0(t_2)$ at each individual temporal point t_2. Here, the maximum value of $\bar{\Omega}_0^2(t_2)$ is $0.36(> 1/3)$. The portion of the signal with $t_2 \in (0.4235, 0.5765)$ falls within the region of $\bar{\Omega}_0^2 > 1/3$ and therefore is unstable. Figure 3 shows the spectrograms of the signal at different values of Z. The spectrograms are generated using a moving Dolph–Chebyshev gating function applied to the signal in the time domain. At $Z = 5,000$, distinct sidebands have already formed at the extremum points of the frequency $\bar{\Omega}_0$. From $Z = 5,000$ to $7,000$, higher order sidebands are quickly generated and widely spread out on the temporal waveform. After $Z = 7,000$, a new signal with a frequency lower than the original signal is generated and becomes dominant. Eventually, the signal in the whole unstable section is replaced by the newly formed signal in the stable region and the higher order sidebands are suppressed in the unstable region. We note that the portions of the signal that were initially in the stable region remain unaffected throughout the entire dynamics.

From the evolution of the solution (25) shown in Figs. 2–3, it is clear that the Eckhaus instability plays a vital role in the dynamics of the signal with either a single frequency offset or

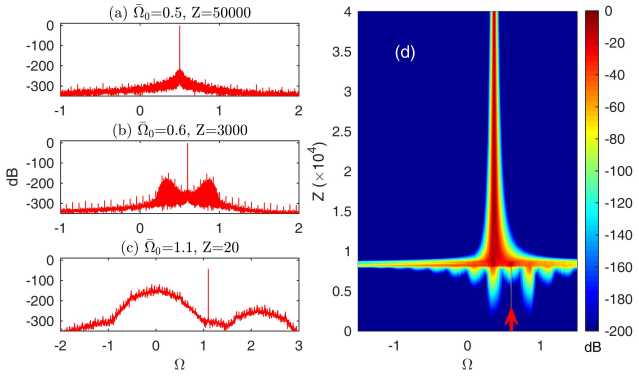

Fig. 2. The spectra of the stationary signals after circulating in the cavity with frequencies in (a) stable region, (b) Eckhaus unstable region and (c) net loss region. (d) The spectrum dynamics of a stationary signal with $\bar{\Omega}_0 = 0.6$, where Eckhaus instability is triggered. The red arrow indicates the frequency of the stationary signal.

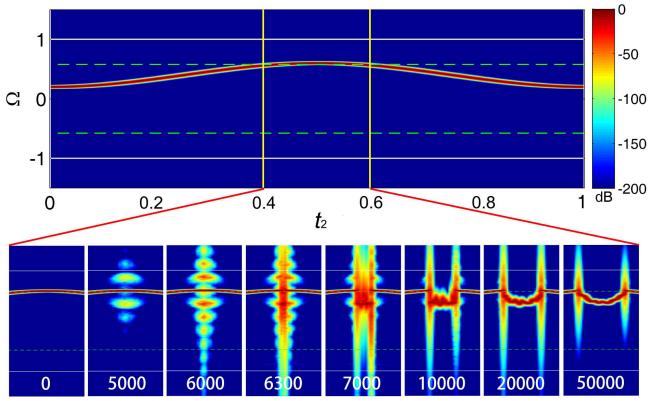

Fig. 3. The spectrograms of the signal with frequency $\bar{\Omega}_0(t_2) = 0.4 - 0.2\cos(2\pi t_2)$ at various values of Z. The top figure shows the entire cavity spectrogram of the signal at $Z = 0$. The dashed lines in the maps indicate the boundaries to trigger Eckhaus instability. The bottom figures show the evolution of the spectrogram in the region of $0.4 < t_2 < 0.6$ from $Z = 0$ to 50,000.

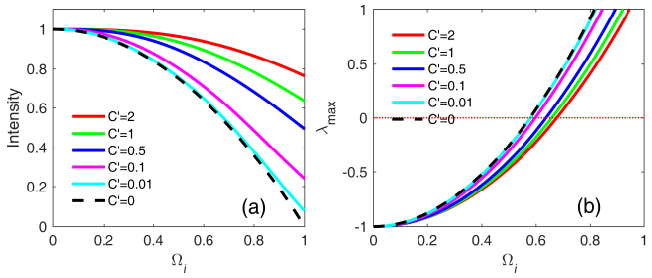

Fig. 4. (a) The intensity evolution of signals propagation with different C'. (b) The maximum eigenvalue λ_{max} of the signals in (a).

a fixed frequency modulation. The portion of the signal with frequencies in the region $\bar{\Omega}_0^2 > 1/3$ becomes unstable and replaced by the generation of a new signal in the stable region. But in a realistic FDML laser, the chirp profile of the signal is not fixed but varying continuously along the propagation, because of a nonzero C', with the system dynamics given by Eq. (14). From $\Omega_i = C'Z - \bar{\Omega}_0$, if C' is nonzero, Ω_i will monotonically increase or decrease with the increase of Z. Such monotonic variation of Ω_i will inevitably push the signal to unstable region.

Figure 4 shows the evolutions of the intensity of Eq. (14) and λ_{max} described by Eq. (21). The intensity and λ_{max} are plotted against the instantaneous frequency Ω_i since it is proportional to Z when $C' \neq 0$, and identical to $\bar{\Omega}_0$ when $C' = 0$. For the curves with $C' \neq 0$, the initial signal at $Z = 0$ are assumed to have $\bar{\Omega}_0 = 0$ and $I_0 = 1$. The dashed curves with $C' = 0$ are for the solution (25). Figure 4(a) shows that for a given value of Ω_i, the intensity of the signal will increase with the increasing value of C' especially for higher values of Ω_i. When $C' < 0.01$, the difference between the dynamically varying chirped solution and the fixed chirped solution indicated by the dashed curve is very small especially in the stable region. In contrast, the intensity curves for higher values of C' deviate significantly from the dashed curve. Besides the deviation of the intensity trace, the stability condition is also affected by the nonzero C', as shown in Fig. 4(b). When C' increases from 0 to 2, the critical point of the instability has been pushed from $\Omega_i = 0.577$ to $\Omega_i = 0.677$. When $C' < 0.01$, the critical point is almost fixed to 0.577 which agrees with the Eckhaus instability criterion.

C. Dynamics in practical laser cavities

To investigate the signal dynamics and the instability in lasers with harmonically swept filter, we consider the same FDML laser cavity described in Fig. 1. The distributed gain coefficient of the cavity is $g_0 = 2.5$ km^{-1} with a flat gain profile. The normalized parameters for such a cavity are $U = 25u$, $Z = 2z$, $\Omega = 12.5\omega$, $t_1 = 0.08t$, $\epsilon = 2.5 \times 10^{-6}$, $t_2 = \epsilon t_1$, and

$$C(t_2) = -1.6 \times 10^{-4} \times \left[\cos^2(2\pi t_2) - 0.8\cos^3(2\pi t_2)\right], \\ C'(t_2) = 10^{-4} \times 3.2\pi \sin(4\pi t_2)\left[1 - 1.2\cos(2\pi t_2)\right], \quad (26)$$

where the maximum value of $|C'|$ is 0.0019. With these normalized parameters, the dynamics of the signal are simulated using Eq. (5). Figures 5 and 6 respectively show the

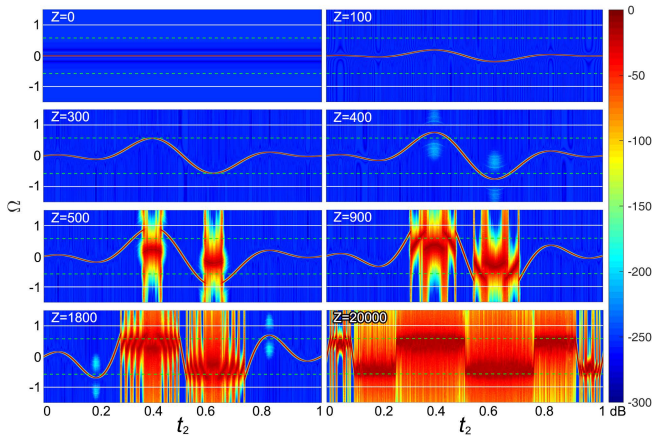

Fig. 5. The spectrograms of the signal in the FDML laser at $Z = 0$, 100, 300, 400, 500, 900, 1800, 20000.

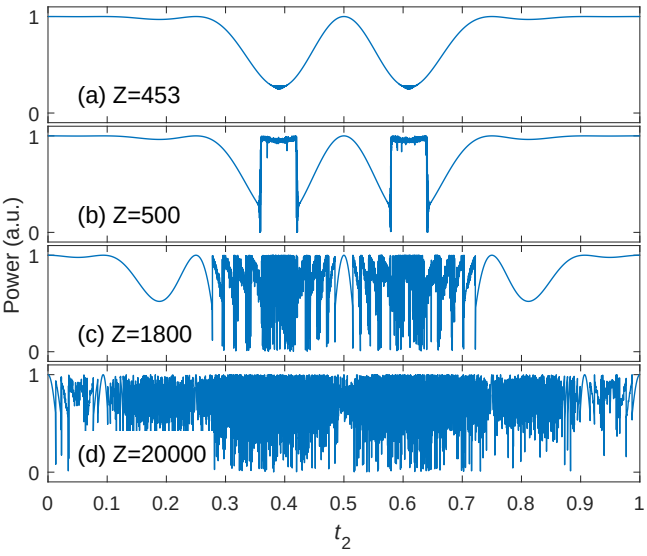

Fig. 6. The waveforms of the signal in the FDML laser at $Z = 453$, 500, 1800, 20000.

spectrograms and the waveforms captured at different Z values in the simulation.

We start the simulation of Eq. (5) from a CW signal with $\bar{\Omega}_0 = 0$. During the propagation along Z, the frequency shift accumulates and continuously pushes part of the spectrogram trace away from the central line $\Omega = 0$, as shown in Fig. 5. In the range of $Z < 300$, the spectrogram trace of the signal remains smooth because the entire signal stays within the stable region of $\Omega^2 < 1/3$. Once the extremum points of the spectrogram trace pass the threshold value of $\Omega^2 = 1/3$ at $Z \approx 303$, sidebands start to grow in the field just outside the stable region but it is too weak to be observed in the early stage. At $Z = 400$, the sidebands are already visible on the spectrogram. The sidebands induce oscillations on the waveform, which is already visible at $Z = 453$ as shown in Fig. 6(a). As the section of the signal located in the unstable region continuously expands, higher order sidebands are also excited. After further signal evolution, e.g., at $Z = 500$, the part of the signals excited the unstable region are replaced

by the new signal generated in the stable region, as shown in Figs. 5 and 6(b). At the same time, the new signals growing in the stable region are also frequency shifted towards the unstable region by the dispersion induced chirp. Eventually, the new signals will leave the stable region and experience its own Eckhaus instability, as shown in Fig. 5 at $Z = 900$. This mechanism of new signals generation in the stable region, frequency shift to the unstable region because of the dispersion effect, and repetition of triggering Eckhaus instability, severely distorts the laser signal. Figures 5 and 6(c) show the multiple order folded spectrogram trace and waveform at $Z = 1800$. After many cycles inside the cavity, e.g., at $Z = 20,000$, the signal has been folded thousands of times and becomes very noisy almost covering the entire region. As shown in the last spectrogram of Fig. 5, most of the signal energy gets distributed near the two boundaries of the stable region with the unstable regions, which means the signal experiences a very high loss when passing through the filter. The signal is completely diffused in the spectrogram, which limits the instantaneous linewidth of the FDML laser. It should be noted that the direction of frequency shift is determined by the sign of C'. Thus the signals with different signs of C' cluster on different sides of the filter.

D. Discussion

From the simulation results reported above with the analytical solution of Eq. (5), it is obvious that the frequency shift caused by the dispersion will continuously push the intracavity signal into unstable region to trigger the Eckhaus instability and generate new signals in the stable region. The simulations results presented in Section III-B clearly show the dynamics in the triggering of Eckhaus instability and generation of new signals in the stable region once the part of existing signal are pushed into the unstable region. The spectrogram evolution and waveforms in Figs. 5 and 6 show how the repetitive triggering of Eckhaus instability destroy the existing signal and introduce the high frequency fluctuations into the waveform.

It should be noted that although we consider only the dispersion induced chirp in our theoretical model (5), such frequency shift may also be induced by other factors in the cavity, such as the jitter of driving signal, thermal or vibration noise to the filter etc. The nonlinear phase distortion caused by the linewidth enhancement factor of the SOA modifies the boundaries of stable region, but will not remove or qualitatively change the evolution of the signals from stable to unstable. We emphasize that the focus of this paper is to delineate the causes of the onset of instability in the laser cavities with harmonically swept filter. We show that the nonlinear phase and the finite recovery time of the gain do not contribute to the triggering of the instability. The complex cavity dynamics after the onset of instability are governed by the dispersion, nonlinear gain and nonlinear phase in the cavity [13], [14], which is not considered in this paper. In applications, it is paramount to keep the operation of the FDML laser in the stable region of stationary solutions to obtain highly coherent output. Currently, such high quality output has only been demonstrated in a laser cavity with fully compensated dispersion with dynamic performance monitoring [15], which agrees with our theoretical analysis that the nonzero dispersion is the fundamental factor that limits the signal quality.

IV. Conclusion

In this paper, we studied the laser cavities with intracavity harmonically swept filters, which could be an FDML laser that is currently used for various applications like OCT. With appropriate model reduction and approximations, we found that the dominant dynamics in the laser cavity can be modeled by an RGLE with a frequency shifting term, which is due to the dispersion of the fiber. We derived the analytic solution of the governing equation and analyzed its stability. We showed that the cavity dispersion introduces a continuous frequency shift (C') to the signal, which pushes the signal outside the stable region and trigger the Eckhaus instability. If the continuous frequency shift is large, the stable region in the frequency domain will be increased. By considering practical parameter values for the FDML laser, we numerically demonstrated that the signal undergoes repeated triggering of Eckhaus instability in the laser cavities by the endless frequency shifting suffered by the signal owing to effects like dispersion. Such mechanism is the root cause of the instability of such laser cavities with harmonically swept filter and nonzero dispersion.

References

[1] R. Huber, K. Taira, M. Wojtkowski, and J. G. Fujimoto, "Fourier Domain Mode Locked Lasers for OCT Imaging at up to 290 kHz Sweep Rates," in *Optical Coherence Tomography and Coherence Techniques II*. Washington, D.C.: OSA, 2005, p. PDA3.

[2] R. Huber, M. Wojtkowski, and J. G. Fujimoto, "Fourier Domain Mode Locking (FDML): A new laser operating regime and applications for optical coherence tomography," *Opt. Express*, vol. 14, no. 8, p. 3225, Apr 2006.

[3] D. Huang, E. Swanson, C. Lin, J. Schuman, W. Stinson, W. Chang, M. Hee, T. Flotte, K. Gregory, C. Puliafito, and A. Et, "Optical coherence tomography," *Science*, vol. 254, no. 5035, pp. 1178–1181, Nov 1991.

[4] J. Fujimoto, "Optical coherence tomography for ultrahigh resolution in vivo imaging." *Nat. Biotechnol.*, vol. 21, no. 11, pp. 1361–1367, 2003.

[5] F. E. Robles, C. Wilson, G. Grant, and A. Wax, "Molecular imaging true-colour spectroscopic optical coherence tomography," *Nat. Photon.*, vol. 5, no. 12, pp. 744–747, 2011.

[6] T. Klein, W. Wieser, R. André, C. Eigenwillig, and R. A. Huber, "Multi-MHz retinal OCT imaging using an FDML laser," in *Biomedical Optics and 3-D Imaging*. Washington, D.C.: OSA, 2012, p. BTu3A.90.

[7] W. Wieser, B. R. Biedermann, T. Klein, C. M. Eigenwillig, and R. Huber, "Multi-Megahertz OCT: High quality 3D imaging at 20 million A-scans and 45 GVoxels per second," *Opt. Express*, vol. 18, no. 14, p. 14685, Jul 2010.

[8] B. R. Biedermann, W. Wieser, C. M. Eigenwillig, T. Klein, and R. Huber, "Dispersion, coherence and noise of Fourier domain mode locked lasers," *Opt. Express*, vol. 17, no. 12, p. 9947, Jun 2009.

[9] D. C. Adler, W. Wieser, F. Trepanier, J. M. Schmitt, and R. A. Huber, "Extended coherence length Fourier domain mode locked lasers at 1310 nm," *Opt. Express*, vol. 19, no. 21, p. 20930, Oct 2011.

[10] W. Wieser, T. Klein, D. C. Adler, F. Trépanier, C. M. Eigenwillig, S. Karpf, J. M. Schmitt, and R. Huber, "Extended coherence length megahertz FDML and its application for anterior segment imaging." *Biomed. Opt. Express*, vol. 3, no. 10, pp. 2647–57, Oct 2012.

[11] C. Jirauschek, B. Biedermann, and R. Huber, "A theoretical description of Fourier domain mode locked lasers." *Opt. Express*, vol. 17, no. 26, pp. 24 013–9, Dec 2009.

[12] S. Todor, B. Biedermann, and R. Huber, "Balance of Physical Effects Causing Stationary Operation of Fourier Domain Mode-Locked Lasers," *J. Opt. Soc. Am. B*, vol. 29, no. 4, p. 656, Mar 2012.

[13] S. Slepneva, B. Kelleher, B. O'Shaughnessy, S. Hegarty, A. Vladimirov, and G. Huyet, "Dynamics of Fourier domain mode-locked lasers," *Optics Express*, vol. 21, no. 16, pp. 19 240–51, Aug 2013.

[14] S. Slepneva, B. O'Shaughnessy, A. G. Vladimirov, S. Rica, E. A. Viktorov, and G. Huyet, "Convective Nozaki-Bekki holes in a long cavity OCT laser," *Optics Express*, vol. 27, no. 11, pp. 16 395–16 404, 2019.
[15] T. Pfeiffer, M. Petermann, W. Draxinger, C. Jirauschek, and R. Huber, "Ultra low noise Fourier domain mode locked laser for high quality megahertz optical coherence tomography," *Biomedical Optics Express*, vol. 9, no. 9, pp. 4130–4148, Sep 2018.
[16] J. Wang, A. Maitra, C. G. Poulton, W. Freude, and J. Leuthold, "Temporal dynamics of the alpha factor in semiconductor optical amplifiers," *Journal of Lightwave Technology*, vol. 25, no. 3, pp. 891–900, 2007.
[17] J. Kevorkian and J. D. Cole, *Multiple Scale and Singular Perturbation Methods*, ser. Applied Mathematical Sciences. New York, NY: Springer, 1996, vol. 114.
[18] F. Li, J. N. Kutz, and P. K. A. Wai, "WKB analysis of Fourier domain mode locked fiber lasers," in *Conference on Lasers and Electro-Optics Pacific Rim (CLEOPR)*, no. 4. IEEE, Jun 2013, pp. WPA–26.
[19] M. Schmidt, T. Pfeiffer, C. Grill, R. Huber, and C. Jirauschek, "Self-stabilization mechanism in ultra-stable Fourier domain mode-locked (FDML) lasers," *OSA Continuum*, vol. 3, no. 6, pp. 1589–1607, Jun 2020.
[20] W. Eckhaus, *Studies in Non-Linear Stability Theory*, ser. Springer Tracts in Natural Philosophy. Berlin, Heidelberg: Springer, 1965, vol. 6.
[21] V. E. Zakharov and L. A. Ostrovsky, "Modulation instability: The beginning," *Physica D*, vol. 238, no. 5, pp. 540–548, 2009.
[22] A. Hasegawa and F. Tappert, "Transmission of stationary nonlinear optical pulses in dispersive dielectric fibers. II. Normal dispersion," *Appl. Phys. Lett.*, vol. 23, no. 4, pp. 171–172, 1973.
[23] N. N. Akhmediev, A. Ankiewicz, and J. M. Soto-Crespo, "Multisoliton Solutions of the Complex Ginzburg-Landau Equation," *Phys. Rev. Lett.*, vol. 79, no. 21, p. 4047, 1997.
[24] N. Akhmediev, J. M. Soto-Crespo, and G. Town, "Pulsating solitons, chaotic solitons, period doubling, and pulse coexistence in mode-locked lasers: Complex Ginzburg-Landau equation approach," *Phys. Rev. E*, vol. 63, no. 5, p. 056602, Apr 2001.
[25] A. Komarov, H. Leblond, and F. Sanchez, "Quintic complex Ginzburg-Landau model for ring fiber lasers," *Phys. Rev. E*, vol. 72, no. 2, p. 025604, Aug 2005.
[26] J. Elgin, J. Gibbon, C. Holmes, J. Molina Garza, and N. Readwin, "Spatial effects and the Eckhaus instability in the laser and Lorenz equations," *Physica D*, vol. 23, no. 1-3, pp. 19–26, Dec 1986.
[27] J. Plumecoq, C. Szwaj, D. Derozier, M. Lefranc, and S. Bielawski, "Eckhaus instability induced by nonuniformities in a laser," *Phys. Rev. A*, vol. 64, no. 6, p. 061801, 2001.
[28] H. Ward, M. Taki, and P. Glorieux, "Secondary transverse instabilities in optical parametric oscillators," *Opt. Lett.*, vol. 27, no. 5, pp. 348–350, Mar 2002.
[29] M. Wolfrum and S. Yanchuk, "Eckhaus instability in systems with large delay," *Phys. Rev. Lett.*, vol. 96, no. 22, p. 220201, 2006.

Feng Li (Member, IEEE, Senior Member, OSA) received the B.Sc and Ph.D degrees from the University of Science and Technology of China, Hefei, China, in 2001 and 2006, respectively. After that, he joined The Hong Kong Polytechnic University, Kowloon, Hong Kong, as a Postdoctoral Fellow. He is currently a Research Assistant Professor in The Hong Kong Polytechnic University. His research interests include fiber lasers including mode locked fiber laser, multi-wavelength fiber laser, wavelength swept laser and its application in bio-photonics; nonlinear optics in optical fiber, micro-resonator/waveguides, including soliton propagation and supercontinuum generation; optoelectronic devices.

Dongmei Huang received her B.Sc degree in 2014 from Huazhong University of Science and Technology, and obtained her M.Sc degree in 2017 from Chongqing University, and obtained her Ph.D degree in 2020 from the Hong Kong Polytechnic University, Kowloon, Hong Kong. She is currently a Research Assistant Professor at Photonics Research Centre of The Hong Kong Polytechnic University. Her research interests include wavelength swept lasers and its applications in optical coherence tomography and optical sensing systems, nonlinear microresonators.

K. Nakkeeran (Fellow IoP, Fellow IET, Senior Member, IEEE, Senior Member, OSA) received the B.Eng. degree from the Coimbatore Institute of Technology, Coimbatore, India, in 1993, and the M. Tech. and Ph.D. degrees from Anna University, Chennai, India, in 1995 and 1998, respectively. In 1999, he joined the Institute of Mathematical Sciences, Chennai, India, where he was a Postdoctoral Fellow for ten months. In 1999, he became a Research Associate with the Department of Physics, University of Burgundy, Dijon, France. In 2002, he became a Postdoctoral Fellow with the Department of Electronic and Information Engineering, The Hong Kong Polytechnic University, Hong Kong. In 2005, he joined the School of Engineering, University of Aberdeen, Aberdeen, U.K., where he has been a Senior Lecturer since 2011. His research interests include solitons, fiber lasers, fiber sensors, modeling and simulations of optical devices, long-haul optical fiber communications, and nonlinear science.

J. Nathan Kutz received the B.Sc degree in physics and mathematics from the University of Washington, Seattle, WA, USA, in 1990, and the Ph.D degree in applied mathematics from Northwestern University, Evanston, IL, USA, in 1994. He is currently a Professor of applied mathematics, an Adjunct Professor of physics and electrical engineering, and a Senior Data Science Fellow with the eScience Institute, University of Washington.

Jinhui Yuan (Senior Member, IEEE, Senior Member, OSA) received the Ph.D degree in physical electronics from the Beijing University of Posts and Telecommunications (BUPT), Beijing, China, in 2011. He is currently a Professor with the Department of Computer and Communication Engineering, University of Science and Technology Beijing (USTB). He was selected as a Hong Kong Scholar with the Photonics Research Centre, Department of Electronic and Information Engineering, The Hong Kong Polytechnic University, in 2013. He has published over 200 papers in the academic journals and conferences. His current research interests include photonic crystal fibers, silicon waveguide, and optical fiber devices. He is a Senior Member of IEEE and a Senior Member of OSA.

P. K. A. Wai (Fellow, IEEE, Fellow, OSA, Fellow, HKAES) received the B.Sc (Hons.) degree from the University of Hong Kong in 1981, and the M.Sc and Ph.D degrees from the University of Maryland, College Park, MD, USA, in 1985 and 1988, respectively. In 1988, he joined Science Applications International Corporation, McLean, VA, USA, where he was a Research Scientist involved with the Tethered Satellite System project. In 1990, he became a Research Associate in the Department of Physics, University of Maryland, College Park, and the Department of Electrical Engineering, University of Maryland, Baltimore County, MD. In 1996, he joined the Department of Electronic and Information Engineering, The Hong Kong Polytechnic University, Kowloon, Hong Kong. He became the Chair Professor of optical communications in 2005. In 2021, he joined Hong Kong Baptist University as President and Chair Professor of photonics in the Department of Physics. His research interests include soliton, fiber lasers, modeling and simulations of optical devices, long-haul optical fiber communications, all-optical packet switching, and network theories. He is an active contributor to the field of photonics and optical communications, having authored or coauthored over 500 international refereed publications.